Parallel metabolic pathway engineering for aerobic 1,2-propanediol production in Escherichia coli

Nonaka, Daisuke ; Hirata, Yuuki ; Kishida, Mayumi ; Mori, Ayana ; Fujiwara, Ryosuke ; Kondo, Akihiko ; Mori, Yutaro ; Noda, Shuhei ;…

(Citation)
Biotechnology Journal,19(8):2400210

(Issue Date)
2024-08

(Resource Type)
journal article

(Version)
Accepted Manuscript

Title

Parallel metabolic pathway engineering for aerobic 1,2-propanediol production in *Escherichia coli*

Daisuke Nonaka[1], Yuuki Hirata[1], Mayumi Kishida[1], Ayana Mori[1], Ryosuke Fujiwara[2] Akihiko Kondo[2,3], Yutaro Mori[1], Shuhei Noda[3,4] and Tsutomu Tanaka[1]*

[1]Department of Chemical Science and Engineering, Graduate School of Engineering, Kobe University, 1-1 Rokkodai-cho, Nada-ku, Kobe, Hyogo 657-8501, Japan

[2]Center for Sustainable Resource Science, RIKEN, 1-7-22, Suehiro-cho, Tsurumi-ku, Yokohama 230-0045, Japan.

[3]Graduate School of Science, Technology and Innovation, Kobe University, 1-1 Rokkodai-cho, Nada-ku, Kobe, Hyogo 657-8501, Japan

[4]PRESTO, Japan Science and Technology Agency (JST), Kawaguchi 332-0012, Saitama, Japan.

*Corresponding Author: tanaka@kitty.kobe-u.ac.jp (T.T.)

Ryosuke Fujiwara ORCID iD: 0000-0003-1549-1087

Akihiko Kondo ORCID iD: 0000-0003-1527-5288

Yutaro Mori ORCID iD: 0000- 0002-5782-9843

Shuhei Noda ORCID iD: 0000-0001-5430-1966

Tsutomu Tanaka ORCID iD: 0000-0002-7397-7360

Running Title: Aerobic 1,2-PDO production using *E. coli*

Abstract

The demand for the essential commodity chemical 1,2-propanediol (1,2-PDO) is on the rise, as its microbial production has emerged as a promising method for a sustainable chemical supply. However, the reliance of 1,2-PDO production in *Escherichia coli* on anaerobic conditions, as enhancing cell growth to augment precursor availability remains a substantial challenge. This study presents glucose-based aerobic production of 1,2-PDO, with xylose utilization facilitating cell growth. We constructed an engineered strain capable of exclusively producing 1,2-PDO from glucose while utilizing xylose to support cell growth. This was accomplished by deleting the *gloA*, *eno*, *eda*, *sdaA*, *sdaB*, and *tdcG* genes for 1,2-PDO production from glucose and introducing the Weimberg pathway for cell growth using xylose. Enhanced 1,2-PDO production was achieved via *yagF* overexpression and disruption of the *ghrA* gene involved in the 1,2-PDO-competing pathway. The resultant strain, PD72, produced 2.48 ± 0.15 g/L 1,2-PDO with a 0.27 ± 0.02 g/g-glucose yield after 72 h cultivation. Overall, this study demonstrates aerobic 1,2-PDO synthesis through the isolation of the 1,2-PDO synthetic pathway from the tricarboxylic acid cycle.

Keywords

1,2-propanediol, *Escherichia coli*, Parallel metabolic pathway engineering, aerobic cultivation, Weimberg pathway, metabolic engineering

1. Introduction

The bio-based chemical industry has received increased attention as the quest for safer and more eco-friendly synthetic processes intensifies, which is attributed to escalating global warming concerns. Much research has implicated the microbial production of chemicals as a viable strategy for achieving the stated quest (Jang et al., 2023). Previous research has successfully produced numerous chemicals, including alcohols, carboxylates, and aromatic compounds, through microbial synthesis. Recent advancements have further broadened the spectrum of chemicals producible in microorganisms (Yang et al., 2020; Choi et al., 2020; Yoo et al., 2022). Considering from the point of view of carbon sources, glucose is a major candidate as a substrate for microbial production (Li et al., 2022; Ding et al., 2022; Wang et al., 2022). To expand the availability of microbial production, the recent studies aimed at the production from a large variety of carbon sources such as glycerol (Lee et al., 2022; Xu et al., 2023; Zhang et al., 2023), galactose (Walls et al., 2022), xylose (Kang et al., 2022). Furthermore, Coelho's group was demonstrated ethylene glycol utilization in oleaginous yeast for glycolic acid production (Carniel et al., 2023). Ethylene glycol was a building block of poly(ethylene terephthalate) (PET). The developments of microbial technology could contribute to the demonstration of sustainable society.

Serving versatile roles, from antifreeze agents to ingredients in food and cosmetics, 1,2-propanediol (1,2-PDO) is also used in polyester resin production. The market value of 1,2-PDO, driven by increasing yearly demand, is expected to surpass $0.398 billion by 2026. The industrial supply route of 1,2-PDO is propylene oxide hydration by the chemical process (Marinas et al., 2015; Tao et al., 2021), which is marked by certain concerns attributed to high-temperature and high-pressure requirements

(Marias et al., 2015). Microbial production of 1,2-PDO is emerging as a promising alternative to traditional supply methods, attracting increased interest.

Bio-based 1,2-PDO production using microorganisms has been investigated in various bacteria and yeasts (Altaras and Cameron, 2000; Niimi et al., 2011; Jo et al., 2023; Islam et al., 2017). In the case of *E. coli*, 1,2-PDO can be synthesized through the methylglyoxal pathway (Altaras and Cameron, 2000). This strategy involves a starting material, dihydroxyacetonephosphate (DHAP), supplied through glycolysis. DHAP is then converted to methylglyoxal by methylglyoxal synthase (MgsA). Methylglyoxal is converted to 1,2-PDO in two ways. First, 1,2-PDO is synthesized from methylglyoxal through two reactions catalyzed by glycerol dehydrogenase (GldA) and L-1,2-propanediol oxidoreductase (FucO) via L-lactaldehyde using 2 NADH molecules (Jain et al., 2015b). Second, methylglyoxal is converted to acetol by aldehyde reductase (YqhD) or alpha-keto reductase (YdjG) using one molecule of NADPH or NADH, respectively. 1,2-PDO can also be synthesized from acetol by GldA using one NADH (Clomburg and Gonzalez, 2011; Jain and Yan, 2011).

Previous studies involving *E. coli* have improved the 1,2-PDO titer by eliminating competing metabolic pathways (Jain et al., 2015ab; Nonaka et al., 2021). 1,2-PDO production in *E. coli* has mostly been conducted under anaerobic conditions to prevent NADH oxidation (Jain et al., 2015a). This condition can result in repressed ATP generation and slower cell growth. Yan's group could overcome the low productivity of 1,2-PDO by introducing an NADH regeneration system using formate dehydrogenase from *Candida boidinii* with 50 mM sodium formate supplementation. Furthermore, overnight anaerobic cultivation in the low phosphate media post-fermentation test improved cell growth. Although these strategies afforded up to 5.13 g/L 1,2-PDO (0.48

g/g glucose) 120 h after IPTG induction, increasing cell growth remains challenging to improve DHAP supply.

A significant issue in metabolic engineering is redirecting carbon flux away from the intended pathway, which can impede the production of target compounds. Intermediates, such as phosphoenolpyruvate (PEP), pyruvate (PYR), and acetyl-CoA, favor the biosynthesis of target chemicals and serve as components of the tricarboxylic acid (TCA) cycle. As a result, the pathways responsible for chemical synthesis from these metabolites often compete with the TCA cycle for carbon flux, leading to diminished yields of the targeted products (Soma et al., 2014). To address this issue, CRISPR interference has been proposed to dynamically alternate between the byproduct synthetic pathway and the production of target chemicals. This system could regulate the expression of enzymes involved in fatty acid synthesis, *fabI* (enoyl-ACP reductase), to balance between cell growth and product formation (Ji et al., 2020). Application of this system markedly enhanced butenoic acid production, achieving a 5.9-fold increase compared to the uninduced control. Despite the utility of the CRISPRi system in rerouting metabolic pathways, the precise timing for activating the switches (e.g., the addition of an inducer to the culture) requires optimization for maximal efficiency.

Modular co-culture engineering is one of promising approaches for achieving high-yield biosynthesis. This technique involves the partitioning of biosynthetic pathways for target compounds across different microbial hosts, each engineered with specific pathways to facilitate the intended biosynthesis. A notable advantage of using multiple strains is the ability to easily regulate metabolic fluxes by adjusting the relative proportions of each strain within the culture (Wang et al., 2020a). By modifying the inoculation ratios of at least two different strains could improve the titer of various

complex chemicals such as rosmarinic acid, acacetin, and raspberry ketone (Li et al., 2019; Wang et al., 2020b; Peng et al., 2023). Furthermore, establishing mutualistic interactions between strains can precisely regulate their ratios. A multi-metabolite cross-feeding (MMCF) strategy is also one of strategies for efficient utilization of substrates for microbial production (Li et al., 2022). In one application, a co-culture of a glutamate auxotrophic mutant strain and a TCA cycle deficient strain resulted in improved production of salidroside, coniferol and silybin/isosilybin.

We have previously reported parallel metabolic pathway engineering (PMPE) as a novel approach to simultaneously utilizing glucose and xylose without compromising cellular growth (Fujiwara et al., 2020). In this strategy, the glycolysis and pentose–phosphate pathway (PPP) are distinctly isolated from the TCA cycle, ensuring that the carbon flux from these pathways, specifically from intermediates such as PEP, does not feed into the TCA cycle. However, in this state, cellular growth is not supported. To address this, we have engineered a xylose catabolic pathway that integrates directly with the TCA cycle, thus avoiding interference with glycolytic and PPP processes. Consequently, this metabolic design channels glucose primarily toward the synthesis of the desired chemicals, whereas xylose is exclusively utilized to sustain cell proliferation. This delineation ensures an efficient bifurcation of metabolic resources, optimizing both product yield and cellular growth. To optimize 1,2-propanediol (1,2-PDO) production, it is essential to repress carbon flux into the TCA cycle by reducing oxygen availability. Under aerobic conditions, the carbon flux toward the TCA cycle is predominant, necessitating a strategic division of metabolic pathways to favor aerobic 1,2-PDO production. PMPE approach ensures that carbon substrates are redirected from the TCA cycle toward the desired biosynthetic pathway, thereby enhancing the yield of 1,2-PDO.

The PMPE strain for shikimate pathway derivative synthesis improved the 1,2-PDO production titer and its yield by 1.40-fold and 11.4-fold (Fujiwara et al., 2020). Although this strain achieved a 0.53 ± 0.16 g/g-glucose 1,2-PDO production yield, the 1,2-PDO titer was still low (0.53 ± 0.01 g/L after 96 h cultivation).

In this study, we engineered a 1,2-PDO-producing strain in alignment with the PMPE concept. This strain could produce 1,2-PDO even under aerobic conditions. The evaluation of xylose assimilation pathways (Dahms and Weimberg pathways), the promotion of xylose utilization, the deletion of byproduct pathways, and the overexpression of 1,2-PDO synthetic genes all resulted in high-yield production of 1,2-PDO under aerobic conditions in engineered *E. coli*. Our findings are poised to markedly benefit the bioproduction of other chemicals, particularly those facing competition at the upstream stages of glycolysis.

2. Materials and Methods

2.1 Strains and plasmids

The strains used in this study are listed in Table 1. The plasmids and primers used in this study are listed in Table S1 and Table S2. *E. coli* MG1655 was used as the host strain. *E. coli* NovaBlue competent cells (Novagen, Cambridge, MA, USA) were used for gene cloning. For PCR, KOD FX Neo (TOYOBO, Osaka, Japan) was used. DNA primers were purchased from the Invitrogen Custom DNA Oligos service (Thermo Fisher Scientific, Tokyo, Japan) or the DNA Custom Synthesis service (FASMAC, Atsugi, Japan).

pZE12-*ccxylB-ccxylC-yagEF* was constructed as follows. The linearized fragment was amplified using inverse PCR using pZE12-*xdh-xylC* as a template with the

primer pair pZ-ccxylB-ccxylC_Inv_ R and pZ-ccxylB-ccxylC_Inv_F. yagEF was amplified using PCR using *E. coli* MG1655 genomic DNA as a template with the primer pair yagE_F and yagF_R. These two linearized fragments were circularized using NEBuilder HiFi DNA Assembly (New England Biolabs Japan, Tokyo, Japan), resulting in pZE12-*ccxylB-ccxylC-yagEF* plasmid.

pZE12-W was constructed as follows. Synthetic genes corresponding to *xylA* and *xylX* from *C. crescentus* were obtained from a commercial source (Invitrogen). The *xylA*, *xylX* and *xylB* gene fragment was amplified using PCR with the *xylA* and *xylX*, *xylB* (Fujiwara et al., 2020) synthetic genes as templates with the primer pair KpnI_CcxylA_F and CcxylA-CcxylX_R, CcxylA-CcxylX_F and CcxylX-CcxylB_R, CcxylX-CcxylB_F and CcxylB_HindIII_R, respectively. The ccxylA-ccxylX gene fragment was amplified using the *ccxylA* and *ccxylX* gene fragments as templates with the primer pair KpnI_CcxylA_F and CcxylX-CcxylB_R. The *ccxylA-ccxylX-ccxylB* gene fragment was amplified using the *ccxylA-ccxylX* gene fragment and *ccxylB* gene fragment as templates with the primer pair KpnI_CcxylA_F and CcxylB_HindIII_R. The amplified fragment was cloned between the *Kpn*I and *Hind*III sites of pZE12-MCS, and the resulting plasmid was designated as pZE12-W.

To construct the pSAK-D1 plasmid, we amplified the insert fragment using PCR with pZE12-*ccxylB-ccxylC-yagEF* as a template. We also used pZ-*Cc_xylB*_F and pZ-yagF_R primers for the pSAK-D1 plasmids. The generated insert fragments were cloned into the *Kpn*I and *Hind*III sites of pSAK, resulting in the pSAK-D1 plasmid. The other plasmids pSAK-D2, pSAK-W, and pSAK-*Bs_mgsA* were constructed using the same procedure.

188 To construct the pZE12-*yagF* plasmid, the DNA sequence of *yagF* was amplified
189 using *E. coli* MG1655 and pZ-yagF_F and pZ-yagF_R primers. This amplified fragment
190 was cloned into the *Kpn*I and *Hind*III sites of pZE12-MCS, resulting in pZE12-*yagF*. The
191 other plasmids pZE12-*yjhG*, pSAK-*gldA*, pSAK-*fucO*, pSAK-*tpiA*, pSAK-*yqhD*, and
192 pSAK-*ydjG* were constructed using the same procedure.
193 pTΔ*eno* was constructed as follows. A plasmid pTargetF was amplified using
194 N20_del_*eno*_F and N20_del_*eno*_R primers. The amplified fragment was self-ligated.
195 The upstream and downstream DNA sequences of *eno* were amplified using the primer
196 pairs Up_del_*eno*_F and Up_del_*eno*_R, Down_del_*eno*_F and Down_del_*eno*_R, with
197 *E. coli* MG1655 as the template. The amplified fragments were fused using overlap
198 extension PCR with the Up_del_*eno*_F and Down_del_*eno*_R primer pairs. The fused
199 fragment was cloned into the *EcoR*I / *Hind*III sites of the plasmid self-ligated, resulting
200 in the pTΔ*eno* plasmid. The other plasmids of the pTarget series pTΔ*sdaB*, pTΔ*tdcG*,
201 pTΔ*dld*, and pTΔ*ghrA* were constructed using the same pTΔ*eno* procedures.
202 The pTΔ*dld*::$P_{A1lacO-1}$-*ccxylAXB* plasmid was constructed using pTΔ*dld*, pSAK-
203 W plasmids and dld_PA1lacO-1_F, dld_PA1lacO-1_R primers. pSAK-W was amplified
204 using PCR with these primers. This fragment was cloned into the SpeI sites of pTΔ*dld*,
205 and the resultant plasmid was pTΔ*dld*::$P_{A1lacO-1}$-*ccxylAXB*.
206
207 **2.2 Media**
208 For pre-culture, LB medium was used. The LB medium included the following
209 (per liter): 10 g tryptone, 5 g yeast extract, and 5 g NaCl. M9Y medium was used for cell
210 growth examination and 1,2-PDO production in 5 mL test tube scale cultures. The M9Y
211 medium comprised carbon source (20 g/L glucose, 10 g/L glucose and 10 g/L xylose, 20

g/L xylose), 5 g/L of yeast extract, 0.1 mM $CaCl_2 \cdot 2H_2O$, 0.01 mM $FeSO_4 \cdot 7H_2O$, 1 mM Mg $SO_4 \cdot 7H_2O$, 10 mg/L of thiamine hydrochloride, 0.5 g/L of NaCl, 6.7 g/L of Na_2HPO_4, 3 g/L of KH_2PO_4, 1 g/L of NH_4Cl, and 0.1 mM IPTG. As needed, ampicillin and/or chloramphenicol were supplemented at the final concentrations of 100 and 30 mg/L, respectively.

2.3 Culture conditions

Engineered strains were inoculated overnight in 4 mL of LB medium at 37°C while being shaken at 220 rpm in a 15 mL test tube. For 1,2-PDO production, this pre-culture was transferred into a 15 mL test tube containing 5 mL of M9Y medium at an initial OD_{600} of 0.1. For cell growth examination, each pre-culture medium was centrifuged at 3000 rpm for 5 min and washed with M9 minimal medium without sugars and metals used for inoculation. The pellet was suspended in fresh medium and seeded into the medium at an initial OD_{600} of 0.1. These test tubes were incubated at 37°C and shaken at 220 rpm.

2.4 Analytical methods

Cell growth was determined by measured OD_{600} using a UVmini-1240 spectrophotometer (Shimadzu Corporation, Kyoto, Japan). Sugars (glucose and xylose) and 1,2-PDO were analyzed using a Prominence HPLC System (Shimadzu) equipped with a Shodex SUGAR KS-801 column (grain diameter, 6 μm; L × I.D., 300 × 8.0 mm; Shodex). The mobile phase was water with a flow rate of 0.8 mL/min rate at 60°C. The HPLC profile was detected using a refractive index detector. Xylonate was analyzed using

a HPLC equipped with a SCR-102H column (7 μm, 8.0 mmID × 300 mmL; Shimadzu) at 50°C. The mobile phase was 5 mM *p*-toluenesulfonic acid with a flow rate of 1.0 mL/min. A conductivity detector was used for monitoring the HPLC profile.

For the NADH/NAD^+ ratio measurement, the samples 48 h after cultivations were analyzed using the EnzyChrom NAD+/NADH Assay Kit (E2ND-100, BioAssay Systems, Hayward, USA), according to the manufacture's procedures.

3. Results and Discussion

3.1. Construction of the engineered strain using glucose for 1,2-PDO production and xylose for cell growth

E coli has endogenous 1,2-PDO production synthetic genes. Notably, 1 mol of 1,2-PDO synthesis in the methylglyoxal pathway requires 2 mol of NADH. Anaerobic cultivation hinders NADH oxidation, thus favoring 1,2-PDO production. However, limiting the oxygen supply reduces cell growth. Under aerobic conditions, DHAP is easily converted to glyceraldehyde 3-phosphate (GAP) for cell maintenance. To solve this dilemma, we aimed to construct an engineered strain capable of producing 1,2-PDO from glucose and consuming xylose for cell growth independently. In this study, we blocked metabolic pathways from glycolytic intermediates upstream of PEP to those downstream of it to improve DHAP availability.

We used the *gloA* gene deficient *E. coli* MG1655Δ*gloA* strain (PD1) as the host strain for 1,2-PDO production (Nonaka et al., 2021). This gene encodes the lactoylglutathione lyase involved in the methylglyoxal assimilation pathway to lactate. *gloA* disruption in *E. coli* favored 1,2-PDO production under anaerobic or microaerobic conditions (Jain et al., 2015b; Nonaka et al., 2021). To separate metabolic pathways, we

selected five genes encoding enolase *eno,* KHG/KDPG aldolase *eda*, L-serine deaminase I *sdaA*, L-serine deaminase II *sdaB*, and L-serine deaminase III *tdcG*. Enolase (Eno) involves in PEP generating reaction from 2-phosphoglycerate. Disrupting the *eno* gene can block the carbon flux to PEP through glycolysis and contribute to improving DHAP availability. Disrupting the *eno* gene in the PD1 strain resulted in a PD2 strain. Although the glyceraldehyde-3-phosphate dehydrogenase A encoded by *gapA* is also a promising target for improving DHAP availability, we could not disrupt the *gapA* gene. KHG/KDPG aldolase encoded by *eda* could convert 2-keto-3-deoxygluconate-6-phosphate to pyruvate and GAP. The expression of xylose dehydrogenase may activate this pyruvate supply route (ED pathway) (Fujiwara et al., 2020). The ED pathway is connected to PPP, and this pathway competes with glycolysis. *eda* disruption in the PD2 strain to eliminate the carbon leak upstream of DHAP yielded a PD3 strain. L-serine deaminases I–III are involved in the serine deamination pathway (Zhang et al., 2014). These enzymes could convert L-serine to pyruvate. L-serine can be synthesized from 3-phosphoglycerate. As this pathway also decreases DHAP availability, we deleted these three enzymes in the PD3 strain, resulting in knockout strain PD4 (Fig. 1).

To test whether the PD4 strain could grow and produce 1,2-PDO in broth containing glucose and xylose, we introduced the Weimberg pathway into the PD4 strain. The Weimberg pathway is found in some bacteria and archaea and comprises five reactions, from xylose to α-ketoglutarate. In the Weimberg pathway, D-xylose is first converted to D-xylonolactone by D-xylose dehydrogenase (XDH). D-xylonolactone turns into D-xylonate catalyzed by xylonolactonase (XLA) or spontaneously. D-xylonate is then converted to 2-Keto-3-deoxy-D-xylonate by D-xylonate dehydratase (D-XAD), and 2-Keto-3-deoxy-D-xylonate is transformed into α-ketoglutarate through two reactions by

2-Keto-3-deoxy-D-xylonate dehydratase (KDXD) and α-ketoglutarate semialdehyde dehydrogenase (KGSADH), respectively (Shen et al., 2020). Through this pathway, a total of 2 mol of NADH is generated from 1 mol of D-xylose with the reactions catalyzed by XDH and KGSADH (Shen et al., 2020). Using the Weimberg pathway could supply carbon from D-xylose to the TCA cycle directly by evading glycolysis. As *E. coli* has endogenous D-XAD (YagF or YjhG) encoded by *yagF* and *yjhG*, *E. coli* could grow from xylose using the Weimberg pathway just by introducing XDH, KDXD, and KGSADH. We used the pSAK-W plasmid having *xylA*, *xylX*, and *xylB* genes from *Caulobacter crescentus*, which encoded KGSADH, KDXD, and XDH, respectively. Incorporating the pSAK-W plasmid into the PD4 strain yielded a PD43 strain. In the medium containing only glucose, the PD43 strain exhibited neither growth nor glucose consumption (Fig. 2a, 2b) but demonstrated initial growth and xylose utilization in the medium containing only xylose, although most xylose was just converted to D-xylonate (XA) (Fig. 2c). This result indicates that PD43 may engage in D-xylose conversion to D-xylonolactone as a strategy to regenerate NADH, albeit this process does not persistently replace the TCA cycle. In a medium containing both glucose and xylose, PD43 exhibited enhanced cell growth relative to those in the other medium and 3.80 g/L glucose and 8.37 g/L xylose were consumed, while XA accumulation was also observed. This result indicates the need to enhance metabolic pathways for XA utilization. Cultivating the PD43 strain in the M9Y medium supplemented with 10 g/L glucose and 10 g/L xylose at 220 rpm. The PD43 strain showed enough growth (Fig. 3a) and yielded 1.48 ± 0.11 g/L of 1,2-PDO, achieving a yield of 0.16 ± 0.01 g/g-glucose after 72 h (Fig. 3b). The PD43 strain also triggered a 5.91 ± 0.16 g/L XA accumulation (Fig. 3c). This strain produced a higher amount of 1,2-PDO than the previously engineered PMPE strain GX1xPD (0.53 ± 0.01 g/L) (Fujiwara et al.,

2020). Although the metabolic design of PD4 was promising, addressing the substantial XA accumulation in the PD43 strain is critical for improving its metabolic efficiency.

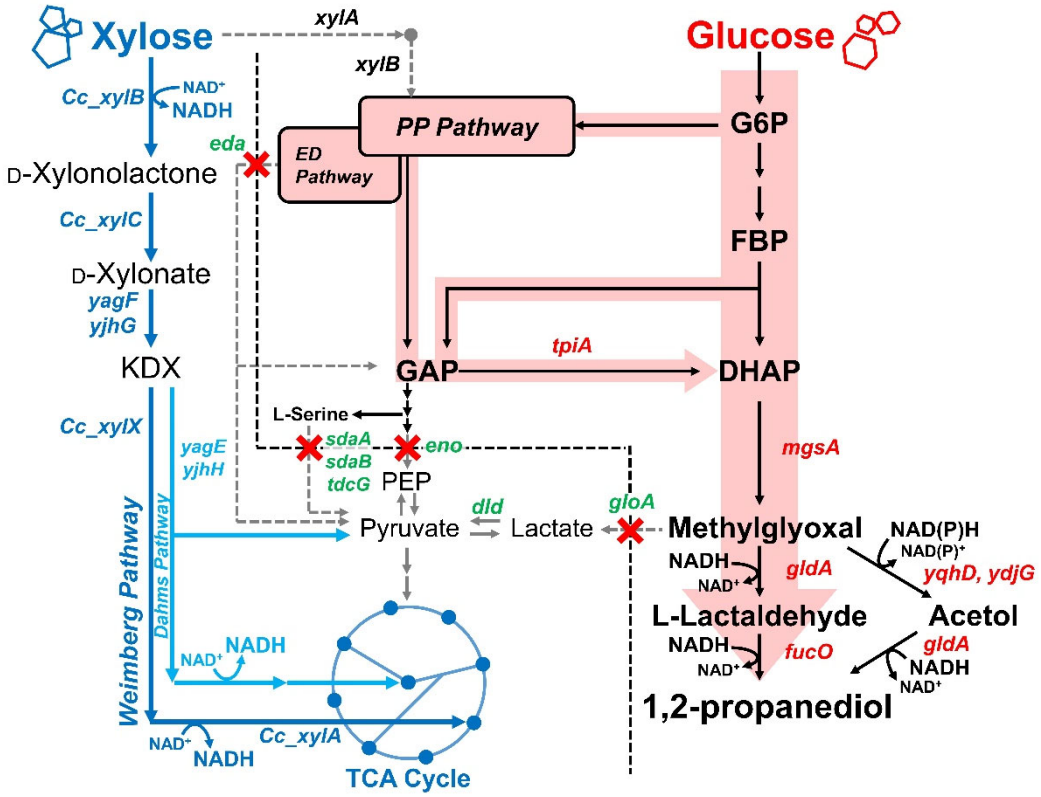

Fig. 1. Metabolic engineering of the *E. coli* strain for the PD4 strain. Red X shows deletion of the *gloA*, *eno*, *eda*, *sdaA*, *sdaB*, and *tdcG* genes. Red indicates genes involved in 1,2-PDO synthesis. Blue indicates genes involved in xylose utilization. G6P, glucose 6-phosphate; FBP, fructose 1,6-bisphosphate; GAP, glyceraldehyde 3-phosphate; DHAP, dihydroxyacetone phosphate; PEP, phosphoenolpyruvate; KDX, 2-Keto-3-deoxy-D-xylonate; PP pathway, pentose–phosphate pathway; ED pathway, Entner–Doudoroff pathway; *gloA*, glyoxalase I; *eno*, enolase; *eda*, KHG/KDPG aldolase; *sdaA*, L-serine deaminase I; *sdaB*, L-serine deaminase II; *tdcG*, L-serine deaminase III; *dld*, D-lactate dehydrogenase; *mgsA*, methylglyoxal synthase; *gldA*, glycerol dehydrogenase; *fucO*, L-

1,2-propanediol oxidoreductase; *tpiA*, triosephosphate isomerase; *yqhD*, aldehyde reductase; *ydjG*, alpha-keto reductase; *yagF, yjhG,* D-xylonate dehydratase; *yagE, yjhH,* keto-pentonate aldolase; *xylA*, D-xylose isomerase; *xylB*, xylulokinase; *Cc_xylB*, D-xylose dehydrogenase from *C. crescentus*; *Cc_xylX*, 2-Keto-3-deoxy-D-xylonate dehydratase from *C. crescentus*; *Cc_xylA*, α-ketoglutarate semialdehyde dehydrogenase from *C. crescentus*.

Table 1. Strains used in this study

Strains	Genotype	Reference
Nova Blue	*endA1*, *hsdR17*,($r_K^-m_K^{+)}$, *supE44 thi-I*, gyrA96, *relA1*, *lac*, *recA1*/F, [*proAB*$^+$, *lacI*qZΔM15,Tn10(Tet R)]	Novagen
MG1655	*Escherichia coli* K-12 MG1655	ATCC
PD1	MG1655 Δ*gloA*	Nonaka et al., 2021
PD2	PD1 Δ*eno*	This study
PD3	PD2 Δ*eda*	This study
PD4	PD3 Δ*sdaA* Δ*sdaB* Δ*tdcG*	This study
PD5	PD4 *dld*::$P_{A1lacO-1}$-*cc_xylAXB*	This study
PD6	PD5 Δ*hchA*	This study
PD7	PD5 Δ*ghrA*	This study
PD8	PD5 Δ*aldA*	This study
PD9	PD6 Δ*ghrA*	This study
PD41	PD4 harboring pSAK-D1 plasmid	This study
PD42	PD4 harboring pSAK-D2 plasmid	This study
PD43	PD4 harboring pSAK-W plasmid	This study
PD50	PD5 harboring pSAK-empty plasmid	This study
PD51	PD5 harboring pZE12 empty plasmid	This study
PD52	PD5 harboring pZE12-*yagF* plasmid	This study
PD53	PD5 harboring pZE12-*yjhG* plasmid	This study
PD521	PD5 harboring pZE12-*yagF* and pSAK plasmids	This study
PD522	PD5 harboring pZE12-*yagF* and pSAK-*Bs_mgsA* plasmids	This study
PD523	PD5 harboring pZE12-*yagF* and pSAK-*gldA* plasmids	This study
PD524	PD5 harboring pZE12-*yagF* and pSAK-*fucO* plasmids	This study
PD525	PD5 harboring pZE12-*yagF* and pSAK-*tpiA* plasmids	This study
PD526	PD5 harboring pZE12-*yagF* and pSAK-*yqhD* plasmids	This study
PD527	PD5 harboring pZE12-*yagF* and pSAK-*ydjG* plasmids	This study
PD528	PD5 harboring pZE12-*yagF* and pSAK-PD plasmids	This study
PD529	PD5 harboring pZE12-*yagF* and pSAK-*Bs_mgsA-yqhD*-	This study

	gldA plasmids	
PD530	PD5 harboring pZE12-*yagF* and pSAK-*Bs_mgsA-ydjG-gldA* plasmids	This study
PD62	PD6 harboring pZE12-*yagF* plasmid	This study
PD72	PD7 harboring pZE12-*yagF* plasmid	This study
PD82	PD8 harboring pZE12-*yagF* plasmid	This study
PD92	PD9 harboring pZE12-*yagF* plasmid	This study

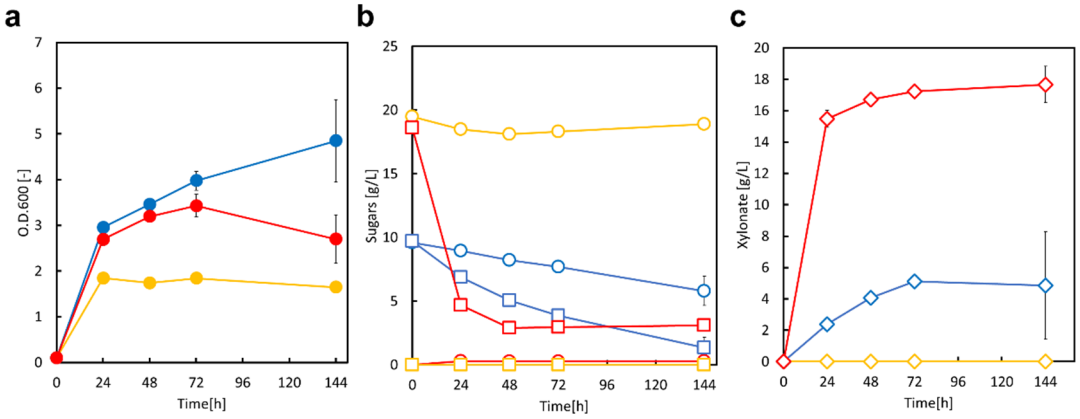

Fig. 2. Culture profiles of the PD43 strain in the M9Y medium containing 20 g/L glucose (yellow), 10g/L glucose and 10g/L xylose (Blue), and 20g/L xylose (Red) using a 15 ml test tube. (a) Cell growth, (b) glucose concentration (circle) and xylose concentration (square), and (c) XA concentration. The data shown are the mean and standard deviations of three independent experiments.

3.2. Evaluation of xylose assimilation pathways for 1,2-PDO production

In metabolic engineering, three well-recognized pathways for xylose assimilation are xylose isomerase, Dahms pathway, and the Weimberg pathways. The latter two pathways intersect at the 2-keto-3-deoxy-D-xylonate juncture. Regarding the Damns pathway, 2-keto-3-deoxy-D-xylonate is converted to glycoaldehyde and pyruvate by keto-pentonate aldolase (YagE or YjhH) encoded by *yagE* or *yjhH* (Bañares et al., 2019). The generated glycoaldehyde is converted to glyoxylate by several enzymes, and the supplied carbon enters the TCA cycle (Fig. 1). While *E. coli* endogenously possesses

343 the xylose isomerase pathway, this pathway does not work well when the Dahms pathway
344 is introduced into an engineered strain (Fujiwara et al., 2020). Therefore, we tested the
345 Dahms pathway instead of the Weimberg pathway in the PD4 strain for 1,2-PDO
346 production.

347 We introduced the Dahms pathway plasmids pSAK-D1 and pSAK-D2 into the
348 PD4 strain. The resultant strains were named PD41 and PD42. pSAK-D1 had *xylB* and
349 *xylC* from *C. crescentus*, *yagE* and *yagF* from *E. coli*. pSAK-D2 had *yjhH* and *yjhG* from
350 *E. coli* instead of *yagE* and *yagF* in pSAK-D1. While YagEF and YjhHG play the same
351 roles in xylose assimilation, those activities are varied (Cabulong et al., 2018). After 72 h
352 of cultivation in M9Y broth containing 10g/L glucose and 10g/L xylose, PD41 and PD42
353 showed 0.31 ± 0.09 g/L and 0.20 ± 0.00 g/L 1,2-PDO (Fig. 3b). XA was not detected in
354 any of the cultivation broths (Fig. 3c). PD41 overexpressing *yagE* and *yagF* afforded
355 greater 1,2-PDO production than PD42 overexpressing *yjhH* and *yjhG*. Paring YagE with
356 YagF proved more effective than paring YjhH with YjhG in terms of decreasing XA
357 accumulation (Cabulong et al., 2018). While our findings did not demonstrate a variance
358 in XA accumulation between PD41 and PD42, disparities in enzyme activities related to
359 D-xylonate and 2-keto-3-deoxy-D-xylonate could influence 1,2-PDO production.
360 Although PD4 produced 1,2-PDO with the Dahms pathway introduced, the PD41 and
361 PD42 strains yielded lower titers than the PD43 strain (Fig. 3b). This result indicates that
362 the Weimberg pathway promotes 1,2-PDO production. The amount of cofactor NADH
363 can influence 1,2-PDO production (Jain et al., 2015a). The Weimberg pathway facilitates
364 a direct carbon supply to the TCA cycle, bypassing pyruvate and glycolate intermediates
365 and potentially enhancing NADH generation from the TCA cycle. We measured the
366 relative $NADH/NAD^+$ ratio in PD41, PD42 and PD43 strain after 48 h cultivation. The

ratio of NADH/NAD^+ in PD43 was slightly higher than other strain (Supplementary Fig 1). To express the Weimberg pathway stably, we integrated $P_{A1lacO-1}$-*Cc_xylAXB* into the *dld* locus of the PD4 strain. The resultant strain was named PD5. The PD5 strain harboring the pSAK-empty vector PD50 showed 1.60 ± 0.19 g/L 1,2-PDO production and 0.19 ± 0.03 g/g-glucose yield after 72 h of cultivation (Fig. 3b). This strain accumulated 0.51 ± 0.36 g/L XA after cultivation (Fig. 3c). Notably, the PD50 strain exhibited reduced XA accumulation compared to the PD43 strain. Directing a greater amount of carbon into the TCA cycle and enhancing NADH production could yield improved 1,2-PDO output. This result indicates that even a single-copy expression of the Weimberg pathway is sufficient, as evidenced by the highest 1,2-PDO production and yield seen in the PD50 strain among the tested strains.

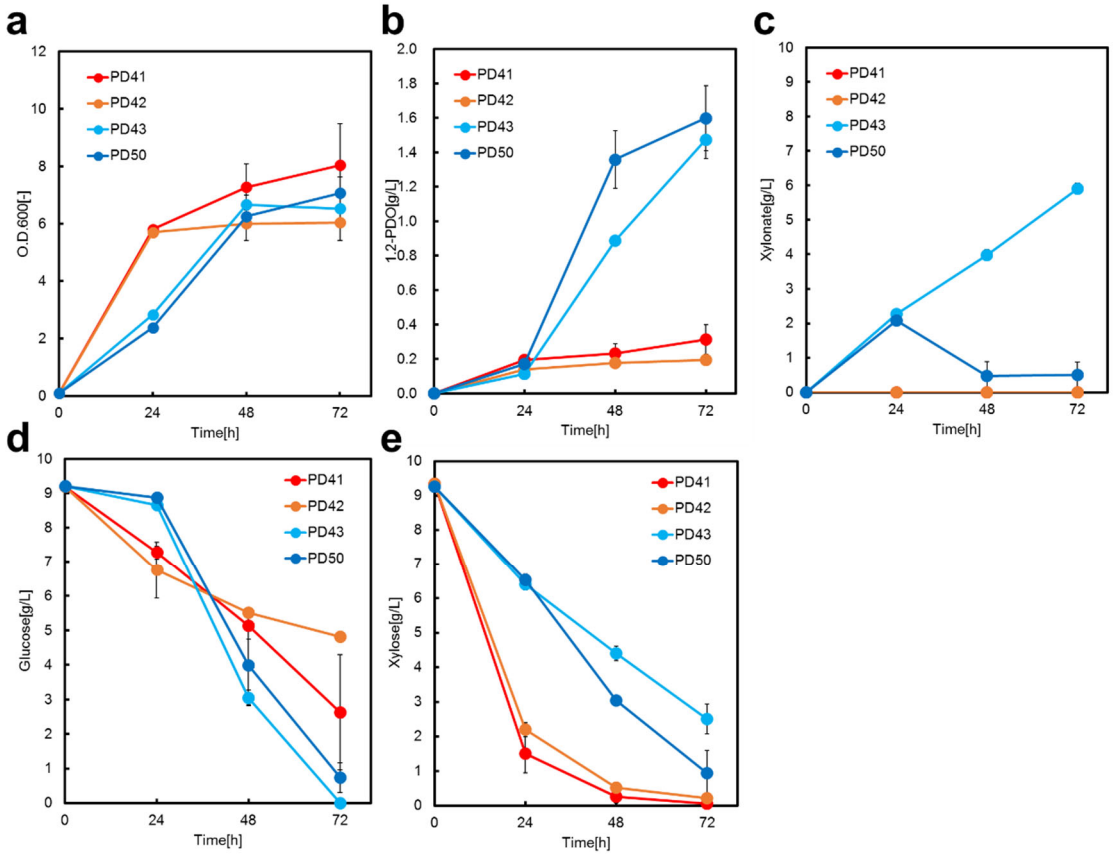

Fig. 3. Cultivation profiles of PD41, PD42, and PD43 harboring pSAK-D1, pSAK-D2, and pSAK-w plasmids, respectively, and PD50 strains harboring pSAK-empty plasmid in M9Y medium containing 10g/L glucose and 10g/L xylose. (a) Cell growth, (b) 1,2-PDO production, (c) XA concentration, (d) glucose concentration, and (e) xylose concentration. The data shown are the mean and standard deviations of three independent experiments.

3.3. Improvement of 1,2-PDO production by modifying the xylose assimilation pathway

The PD50 strain demonstrated increased 1,2-PDO production and reduced XA accumulation. This result suggests that fine-tuning gene expression levels is pivotal for optimizing xylose utilization. Enhancing the xylose assimilation pathway could further increase 1,2-PDO production attributed to increased NADH generation via the TCA cycle. Enhancing the expression of YagF and YjhG could lead to a more effective utilization of D-xylonate. We promoted D-xylonate assimilation through the overexpression of the D-XADs YagF or YjhG. The overexpression of D-XAD *yagF* and *yjhG* contributes to reduced D-xylonate accumulation (Cabulong et al., 2018). Incorporating the constructed pZE12-*yagF* and pZE12-*yjhG* plasmids into the PD5 strain afforded the PD52 and PD53 strains, respectively. As a control, we also introduced a pZE12-empty vector into the PD5 strain, resulting in the PD51 strain. After 72 h cultivations, PD52 showed 2.04 ± 0.10 g/L 1,2-PDO production with a yield of 0.24 ± 0.01 g/g-glucose (Fig. 4b, 4c). This result indicates that *yagF* overexpression effectively favors 1,2-PDO production. A previous study revealed that the activity of YagF on D-xylonate was 2.56 times higher than that of YjhG, according to enzyme assays (Cabulong et al., 2018). The overexpression of D-

XAD YagF improved carbon utilization from xylose to the TCA cycle and contributed to the cofactor balance.

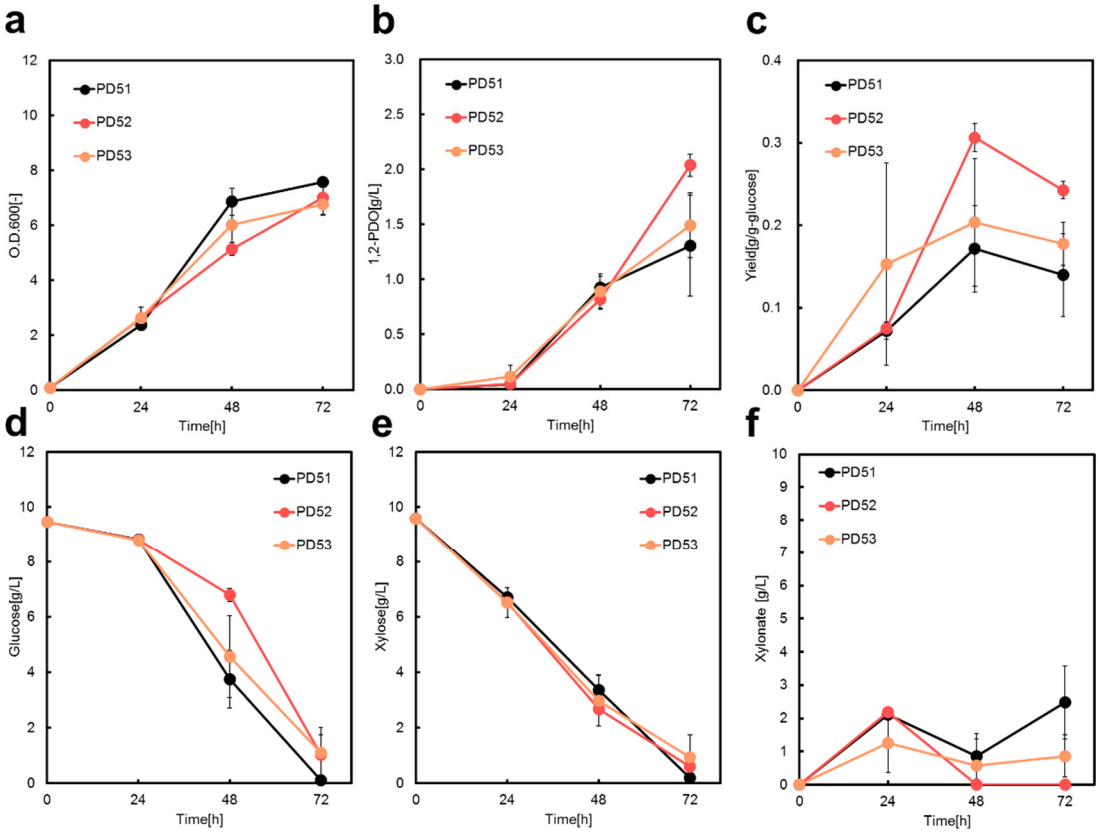

Fig. 4. Culture profiles using the PD51, PD52, and PD53 in M9Y medium containing 10g/L glucose and 10g/L xylose for 72 h cultivation. (a) Cell growth, (b) 1,2-PDO production, (c) 1,2-PDO yield from the consumed glucose, (d) glucose concentration, (e) xylose concentration and (f) XA concentration. The data shown are the mean and standard deviations of three independent experiments.

3.4. Overexpression of genes involved in 1,2-PDO production from glucose

To enhance the 1,2-PDO synthetic pathway, we overexpressed *gldA*, *fucO*, *tpiA*, *yqhD*, *ydjG*, endogenous genes and *mgsA* from *B. subtilis* in PD5. These genes encode glycerol dehydrogenase, L-1,2-propanediol oxidoreductase, triosephosphate isomerase,

aldehyde reductase, alpha-keto reductase and methylglyoxal synthase, respectively. The methylglyoxal synthase from *B. subtilis* had higher activity to DHAP than endogenous *E. coli* methyglyoxal synthase (Jain and Yan, 2011). To improve DHAP availability, we chose *mgsA* from *B. subtilis* instead of endogenous *mgsA* (Nonaka et al., 2021).

We introduced pSAK-empty vector, pSAK-*Bs_mgsA*, pSAK-*gldA*, pSAK-*fucO*, pSAK-*tpiA*, pSAK-*yqhD* or pSAK-*ydjG* into a PD52 strain. The resultant strains were named PD521, PD522, PD523, PD524, PD525, PD526, and PD527. After 72 h of cultivation in the M9Y medium, these strains produced 2.03 ± 0.70 g/L, 2.27 ± 0.13 g/L, 0.70 ± 0.10 g/L, 1.90 ± 0.12 g/L, 2.15 ± 0.32 g/L, 1.46 ± 0.25 g/L, and 1.68 ± 0.31 g/L 1,2-PDO, respectively (Fig. 5a). The yields of 1,2-PDO in those strains were 0.25 ± 0.05, 0.26 ± 0.01, 0.13 ± 0.00, 0.32 ± 0.01, 0.24 ± 0.04, 0.28 ± 0.06, and 0.29 ± 0.04 g/g-glucose (Fig. 5b). Although *Bs_mgsA* and *tpiA* overexpression slightly improved 1,2-PDO production, the yield of 1,2-PDO was similar to the control strain. The enhancement in the 1,2-PDO yield resulting from *fucO* overexpression suggests that the bottleneck in the 1,2-PDO synthesis pathway may lie in the final reaction catalyzed by FucO. However, the PD524 strain showed lower glucose consumption than the PD521. Enhancing glucose consumption in the PD524 strain through genetic manipulation could lead to further improvements in 1,2-PDO productivity. A previous study indicated that the enzyme FucO was affected by oxidative stress and its activity weakened under aerobic conditions. Two mutations of FucO showed higher propanediol oxidoreductase activity under aerobic conditions, compared to the native enzyme (Lu et al., 1998). While, to our knowledge, this enzyme has not yet been applied to 1,2-PDO production, variants of FucO hold promise for enhancing 1,2-PDO productivity. For an alternative pathway via acetol, *yqhD* or *ydjG* overexpression had a significant effect on the 1,2-PDO titer. This result indicates

that the route via lactaldehyde is important for 1,2-PDO synthesis. Although the *gldA* gene is involved in both pathways, *gldA* overexpression had a negative effect on 1,2-PDO production (Fig. 5a).

We introduced pSAK-PD, pSAK-*Bs_mgsA-yqhD-gldA* or pSAK-*Bs_mgsA-ydjG-gldA*, which contained a set of 1,2-PDO synthetic genes, into PD52 strain. These strain were named PD528, PD529 and PD530, respectively. The 1,2-PDO production titer in PD528-530 strain was comparable to or lower than that in PD521 (Fig. 5a).

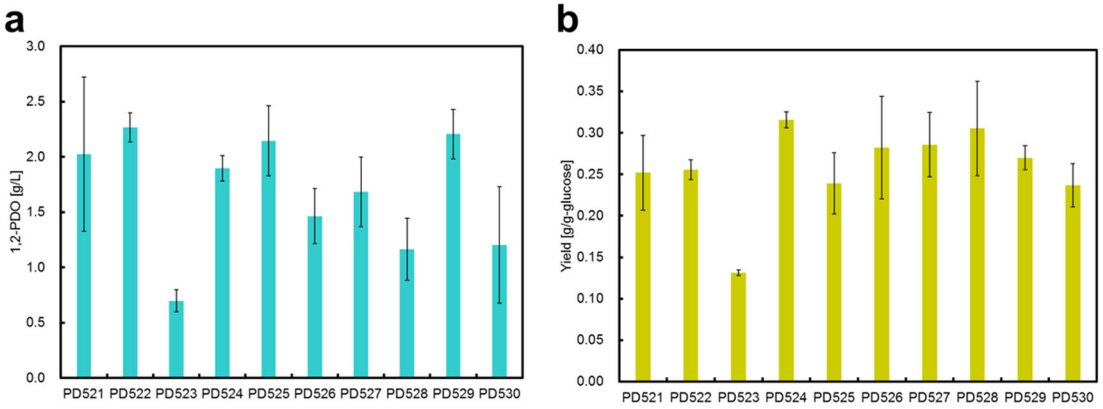

Fig. 5. Culture profiles using the PD521-530 strains in M9Y medium containing 10g/L glucose and 10g/L Xylose after 72 h cultivation. (a) 1,2-PDO production, (b) yields. The data shown are the mean and standard deviations of three independent experiments.

3.5. Improvement of 1,2-PDO production by deletion of carbon leakage

Overexpressing genes within the 1,2-PDO synthesis pathway may not markedly enhance 1,2-PDO production. We speculated that carbon leakage to byproducts from intermediates in the 1,2-PDO synthesis pathway might have occurred. Methylglyoxal and L-lactaldehyde can be converted to byproducts by glyoxalase III and Hsp31 molecular chaperone (encoded by *hchA*), glyoxylate/hydroxypyruvate reductase (encoded by *ghrA*), and aldehyde dehydrogenase A (encoded by *aldA*) (Clomburg and Gonzalez, 2011;

Nonaka et al., 2021). Glyoxalase III and glyoxylate/hydroxypyruvate reductase could convert methylglyoxal to lactate and D-lactaldehyde, respectively. An aldehyde dehydrogenase A is involved in the consumption of L-lactaldehyde, an intermediate of the 1,2-PDO pathway. This enzyme can aid pyruvate formation from methylglyoxal (Fig. 6a). *hchA* and *aldA* deletions improved 1,2-PDO production in an engineered strain under microaerobic conditions (Nonaka et al., 2021). In this study, disrupting *hchA*, *ghrA*, and *aldA* in the PD5 strain yielded PD6, PD7, and PD8 strains, respectively. The resultant strains PD62, PD72, and PD82 harboring pZE12-*yagF* showed 2.33 ± 0.06, 2.48 ± 0.15, and 1.51 ± 0.10 g/L 1,2-PDO after 72-h cultivation, with yields from glucose as 0.29 ± 0.05, 0.27 ± 0.02, and 0.19 ± 0.02 g/g-glucose (Fig. 6b, 6c). Disrupting *hchA* or *ghrA* genes slightly improved 1,2-PDO production and the yield from glucose. These results indicate that diminishing the diversion of methylglyoxal into byproduct pathways can improve 1,2-PDO production, while the lack of the *aldA* gene leads to reduced 1,2-PDO production. The enzymatic reactions facilitated by *aldA* are pivotal for generating NADH, a coenzyme essential for 1,2-PDO biosynthesis. Therefore, *aldA* disruption adversely impacts the redox balance within the engineered strain, ultimately failing to increase 1,2-PDO production levels. This shows the critical role of *aldA* in maintaining the cellular redox state and its direct influence on 1,2-PDO production.

According to the above results, we constructed PD9 by disrupting *hchA* and *ghrA* genes in PD5 strain. PD92 strain harboring pZE12-*yagF* showed lower 1,2-PDO production than PD72 strain (Fig. 6b). The combination of disruptions of *hchA* and *ghrA* did not contribute to the improvement of 1,2-PDO production.

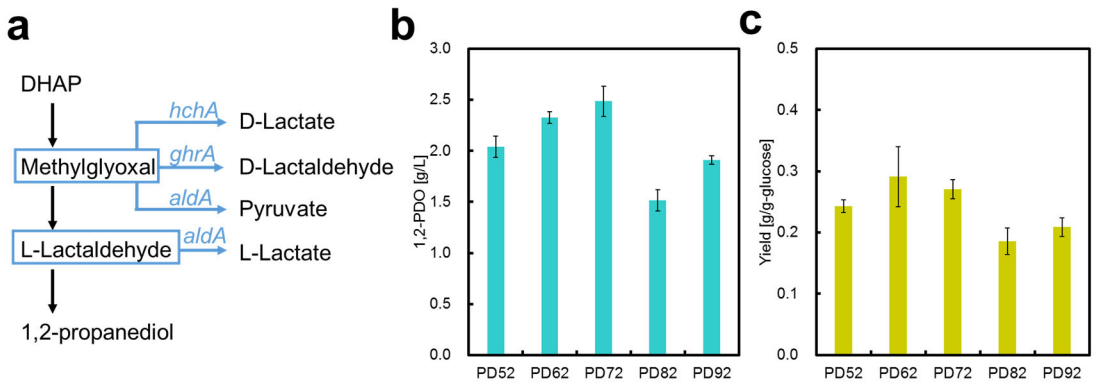

Fig. 6 (a) Byproduct synthetic pathway competing with the 1,2-PDO synthetic pathway. *hchA*, glyoxalase III and Hsp31 molecular chaperone; *ghrA*, glyoxylate/hydroxypyruvate reductase; *aldA*, aldehyde dehydrogenase A. (b)(c) Culture profiles using PD62, PD72, PD82 and PD92 in the M9Y medium containing 10g/L glucose and 10g/L Xylose after 72 h cultivation. (b) 1,2-PDO production, and (c) 1,2-PDO yield from consumed glucose. The data shown are the mean and standard deviations of three independent experiments.

4. Conclusion

In this study, we demonstrated aerobic 1,2-PDO production by decoupling the metabolic pathways for target compound production from glucose and fueling cell growth by xylose utilization. The efficient use of xylose through the Weimberg pathway contributed to improving 1,2-PDO production. *yagF* overexpression in PD5 produced 2.04 ± 0.10 g/L 1,2-PDO with a yield of 0.24 ± 0.01 g/g-glucose. By optimizing the 1,2-PDO synthesis pathway and inhibiting byproduct generation via the methylglyoxal pathway, we achieved an improved 1,2-PDO titer of up to 2.48 ± 0.15 g/L. The summarized table of 1,2-PDO production in previous studies was shown in Table S3. This titer was higher than that in previous study under microaerobic cultivation. Further optimization of both glucose and xylose utilization pathways could improve aerobic 1,2-

PDO production. Our findings offer valuable insights for synthesizing other chemicals whose production is constrained by competition with central metabolic pathways.

Authorship contribution statement

Daisuke Nonaka: Conceptualization, Investigation, Writing - original draft. Yuuki Hirata: Investigation. Mayumi Kishida: Investigation. Ayana Mori: Investigation. Ryosuke Fujiwara: Conceptualization, Investigation, Writing - review & editing. Akihiko Kondo: Resources. Yutaro Mori: Writing - review & editing. Shuhei Noda: Conceptualization, Writing - review & editing. Tsutomu Tanaka: Conceptualization, Investigation, Writing - review & editing, Funding acquisition, Project administration.

Acknowledgements

The authors would like to thank Enago (www.enago.com) for English language editing.

Conflict of interest statement

The authors have no conflict of interest to declare.

Data availability statement

The data that support the findings of this study are available from the corresponding author upon reasonable request.

Funding information

This work was supported by Japan Society for the Promotion of Science (JSPS) Grant-in-Aid for JSPS Research Fellow (Grant Number JP22KJ2279) (to D.N.) Grants-in-Aid for Scientific Research (B) (Grant Number JP22H01885) (to S.N.), Grant-in-Aid for Transformative Research Areas (Grant Number 23H04565) (to S.N.) and by Japan Science and Technology Agency (JST) through the Precursory Research for Embryonic

520 Science and Technology (PRESTO) grant number JPMJPR22N9 (to S.N.) and Grants-in-
521 Aid for Scientific Research (B) (Grant Number JP22H01880).

522

523 **References**

524 Altaras, N. E., & Cameron, D. C. (2000). Enhanced production of (R)-1,2-
525 propanediol by metabolically engineered *Escherichia coli*. *Biotechnology Progress*, *16,*
526 940–946. *doi:*10.1021/bp000076z

527 Bañares, A. B., Valdehuesa, K. N. G., Ramos, K. R. M., Nisola, G. M., Lee, W.
528 K., & Chung, W. J. (2019). Discovering a novel D-xylonate-responsive promoter: the
529 PyjhI-driven genetic switch towards better 1,2,4-butanetriol production. *Applied*
530 *Microbiology and Biotechnology, 103,* 8063–8074. *doi:*10.1007/s00253-019-10073-0

531 Cabulong, R. B., Lee, W. K., Bañares, A. B., Ramos, K. R. M., Nisola, G. M.,
532 Valdehuesa, K. N. G., & Chung, W. J. (2018). Engineering Escherichia coli for glycolic
533 acid production from D-xylose through the Dahms pathway and glyoxylate bypass.
534 *Applied Microbiology and Biotechnology, 102,* 2179–2189. *doi:*10.1007/s00253-018-
535 8744-8

536 Carniel, A., Santos, A. G., Chinelatto, L. S., Júnior, Castro, A. M., & Coelho, M.
537 A. Z. (2023). Biotransformation of ethylene glycol to glycolic acid by *Yarrowia lipolytica*:
538 A route for poly(ethylene terephthalate) (PET) upcycling. *Biotechnology Journal*, *18(6)*,
539 e2200521. *doi:*10.1002/biot.202200521

540 Choi, K. R., Jiao, S., & Lee, S. Y. (2020). Metabolic engineering strategies
541 toward production of biofuels. *Current Opinion in Chemical Biology, 59,* 1–14.
542 *doi:*10.1016/j.cbpa.2020.02.009

543 Clomburg, J. M., & Gonzalez, R. (2011). Metabolic engineering of *Escherichia*

544 *coli* for the production of 1,2-propanediol from glycerol. *Biotechnology and*
545 *Bioengineering, 108,* 867–879. *doi:*10.1002/bit.22993
546 Ding, W., Meng, Q., Dong, G., Qi, N., Zhao, H., & Shi, S. (2022). Metabolic
547 engineering of threonine catabolism enables *Saccharomyces cerevisiae* to produce
548 propionate under aerobic conditions. *Biotechnology Journal*, *17(3)*, e2100579.
549 *doi:*10.1002/biot.202100579
550 Fujiwara, R., Noda, S., Tanaka, T., & Kondo, A. (2020). Metabolic engineering
551 of *Escherichia coli* for shikimate pathway derivative production from glucose–xylose co-
552 substrate. *Nature Communications, 11,* 279. *doi:*10.1038/s41467-019-14024-1
553 Islam, Z. U., Klein, M., Aßkamp, M. R., Ødum, A. S. R., & Nevoigt, E. (2017)
554 A modular metabolic engineering approach for the production of 1,2-propanediol from
555 glycerol by Saccharomyces cerevisiae. *Metabolic Engineering, 44,* 223–235.
556 *doi:*10.1016/j.ymben.2017.10.002
557 Jain, R., & Yan, Y. (2011). Dehydratase mediated 1-propanol production in
558 metabolically engineered *Escherichia coli*. *Microbial Cell Factories*, *10*, 97.
559 *doi:*10.1186/1475-2859-10-97
560 Jain, R., Huang, J., Yuan, Q., & Yan, Y. (2015). Engineering microaerobic
561 metabolism of *E. coli* for 1,2-propanediol production. *Journal of Industrial Microbiology*
562 *and Biotechnology, 42,* 1049–1055. *doi:*10.1007/s10295-015-1622-9
563 Jain, R., Sun, X., Yuan, Q., & Yan, Y. (2015). Systematically engineering
564 *Escherichia coli* for enhanced production of 1,2-propanediol and 1-propanol. *ACS*
565 *Synthetic Biology, 4,* 746–756. *doi:*10.1021/sb500345t
566 Jang, W. D., Kim, G. B., & Lee, S. Y. (2023). An interactive metabolic map of
567 bio-based chemicals. *Trends in Biotechnology*, *41(1)*, 10–14.

*doi:*10.1016/j.tibtech.2022.07.013

Ji, X., Zhao, H., Zhu, H., Zhu, K., Tang, S. Y., & Lou, C. (2020). CRISPRi/dCpf1-mediated dynamic metabolic switch to enhance butenoic acid production in *Escherichia coli*. *Applied Microbiology and Biotechnology, 104,* 5385–5393. *doi:*10.1007/s00253-020-10610-2

Jo, M. H., Ju, J. H., Heo, S. Y., Cho, J., Jeong, K. J., Kim, M. S., Kim, C. H., & Oh, B. R. (2023). Production of 1,2-propanediol from glycerol in *Klebsiella pneumoniae* GEM167 with flux enhancement of the oxidative pathway. *Biotechnology for Biofuels and Bioproducts, 16,* 18. *doi:*10.1186/s13068-023-02269-4

Kang, N. K., Lee, J. W., Ort, D. R., & Jin, Y.-S. (2022). L-malic acid production from xylose by engineered *Saccharomyces cerevisiae*. *Biotechnology Journal*, *17(3)*, e2000431. *doi:*10.1002/biot.202000431

Li, B., Zhang, B., Wang, P., Cai, X., Tang, Y.-Q., Jin, J.-Y., Liang, J.-X., Liu, Z.-Q., & Zheng, Y.-G. (2022). Targeting metabolic driving and minimization of by-products synthesis for high-yield production of D-pantothenate in *Escherichia coli*. *Biotechnology Journal*, *17(1)*, e2100431. *doi:*10.1002/biot.202100431

Li, X., Zhou, Z., Li, W., Yan, Y., Shen, X., Wang, J., Sun, X., & Yuan, Q. (2022). Design of stable and self-regulated microbial consortia for chemical synthesis. *Nature Communications*, *13*(1), 1554. *doi:*10.1038/s41467-022-29215-6

Li, Z., Wang, X., & Zhang, H. (2019). Balancing the non-linear rosmarinic acid biosynthetic pathway by modular co-culture engineering. *Metabolic Engineering*, *54*, 1–11. *doi:*10.1016/j.ymben.2019.03.002

Lee, H.-J., Shin, D. J., Han, K., Chin, Y.-W., Park, J. P., Park, K., Choi, C.-H., Park, B.-R., Kim, S.-J., & Kim, S.-K. (2022). Simultaneous production of 2’-

592 fucosyllactose and difucosyllactose by engineered *Escherichia coli* with high secretion
593 efficiency. *Biotechnology Journal*, *17(3)*, e2100629. *doi:*10.1002/biot.202100629
594 Lu, Z., Cabiscol, E., Obradors, N., Tamarit, J., Ros, J., Aguilar, J., & Lin, E. C.
595 C. (1998). Evolution of an *Escherichia coli* protein with increased resistance to oxidative
596 stress. *The Journal of Biological Chemistry, 273,* 8308–8316.
597 *doi:*10.1074/jbc.273.14.8308
598 Marinas, A., Bruijnincx, P., Ftouni, J., Urbano, F. J., & Pinel, C. (2015).
599 Sustainability metrics for a fossil- and renewable-based route for 1,2-propanediol
600 production: A comparison. *Catalysis Today, 239,* 31–37.
601 *doi:*10.1016/j.cattod.2014.02.048
602 Niimi, S., Suzuki, N., Inui, M., & Yukawa, H. (2011). Metabolic engineering of
603 1,2-propanediol pathways in *Corynebacterium glutamicum*. *Applied Microbiology and*
604 *Biotechnology, 90,* 1721–1729. *doi:*10.1007/s00253-011-3190-x
605 Nonaka, D., Fujiwara, R., Hirata, Y., Tanaka, T., & Kondo, A. (2021). Metabolic
606 engineering of 1,2-propanediol production from cellobiose using beta-glucosidase-
607 expressing *E. coli*. *Bioresource Technology, 329,* 124858.
608 *doi:*10.1016/j.biortech.2021.124858
609 Peng, H., Chen, R., Shaw, W. M., Hapeta, P., Jiang, W., Bell, D. J., Ellis, T., &
610 Ledesma-Amaro, R. (2023). Modular Metabolic Engineering and Synthetic Coculture
611 Strategies for the Production of Aromatic Compounds in Yeast. *ACS Synthetic Biology*.
612 *doi:*10.1021/acssynbio.3c00047
613 Shen, L., Kohlhaas, M., Enoki, J., Meier, R., Schönenberger, B., Wohlgemuth,
614 R., Kourist, R., Niemeyer, F., van Niekerk, D., Bräsen, C., Niemeyer, J., Snoep, J., &
615 Siebers, B. (2020). A combined experimental and modelling approach for the Weimberg

pathway optimisation. *Nature Communications, 11,* 1098. *doi:*10.1038/s41467-020-14830-y

Soma, Y., Tsuruno, K., Wada, M., Yokota, A., & Hanai, T. (2014). Metabolic flux redirection from a central metabolic pathway toward a synthetic pathway using a metabolic toggle switch. *Metabolic Engineering, 23,* 175–184. *doi:*10.1016/j.ymben.2014.02.008

Tao, Y. M., Bu, C. Y., Zou, L. H., Hu, Y. L., Zheng, Z. J., & Ouyang, J. (2021). A comprehensive review on microbial production of 1,2-propanediol: micro-organisms, metabolic pathways, and metabolic engineering. *Biotechnology for Biofuels, 14,* 216. *doi:*10.1186/s13068-021-02067-w

Walls, L. E., Martinez, J. L., Del Rio Chanona, E. A., & Rios-Solis, L. (2022). Definitive screening accelerates Taxol biosynthetic pathway optimization and scale up in *Saccharomyces cerevisiae* cell factories. *Biotechnology Journal*, *17(1)*, e2100414. *doi:*10.1002/biot.202100414

Wang, R., Zhao, S., Wang, Z., & Koffas, M. A. (2020). Recent advances in modular co-culture engineering for synthesis of natural products. *Current Opinion in Biotechnology*, *62*, 65–71. *doi:*10.1016/j.copbio.2019.09.004

Wang, X., Shao, A., Li, Z., Policarpio, L., & Zhang, H. (2020). Constructing E. coli Co-Cultures for De Novo Biosynthesis of Natural Product Acacetin. *Biotechnology Journal*, *15*(9), e2000131. *doi:*10.1002/biot.202000131

Wang, Y., Xu, J., Jin, Z., Xia, X., & Zhang, W. (2022). Improvement of acetyl-CoA supply and glucose utilization increases l-leucine production in *Corynebacterium glutamicum*. *Biotechnology Journal*, *17(8)*, e2100349. *doi:*10.1002/biot.202100349

Xu, J.-M., Wu, Z.-S., Zhao, K.-J., Xi, Z.-J., Wang, L.-Y., Cheng, F., Xue, Y.-P.,

& Zheng, Y.-G. (2023). IPTG-induced high protein expression for whole-cell biosynthesis of L-phosphinothricin. *Biotechnology Journal*, *18(9)*, e2300027. *doi:*10.1002/biot.202300027

Yang, D., Park, S. Y., Park, Y. S., Eun, H., & Lee, S. Y. (2020). Metabolic engineering of *Escherichia coli* for natural product biosynthesis. *Trends in Biotechnology, 38,* 745–765. *doi:*10.1016/j.tibtech.2019.11.007

Yoo, J. I., Sohn, Y. J., Son, J., Jo, S. Y., Pyo, J., Park, S. K., Choi, J.-I., Joo, J. C., Kim, H. T., & Park, S. J. (2022). Recent advances in the microbial production of C4 alcohols by metabolically engineered microorganisms. *Biotechnology Journal*, *17(3)*, e2000451. *doi:*10.1002/biot.202000451

Zhang, H., Zhao, A., Qu, L., Xiong, W., Alam, M. A., Miao, J., Wang, W., Xu, J., & Lv, Y. (2023). Engineering an efficient whole-cell catalyst for d-allulose production from glycerol. *Biotechnology Journal*, *18(7)*, e2200600. *doi:*10.1002/biot.202200600

Zhang, Y., Lin, Z., Liu, Q., Li, Y., Wang, Z., Ma, H., Chen, T., & Zhao, X. (2014). Engineering of serine-deamination pathway, Entner-Doudoroff pathway and pyruvate dehydrogenase complex to improve poly(3-hydroxybutyrate) production in *Escherichia coli*. *Microbial Cell Factories, 13,* 172. *doi:*10.1186/s12934-014-0172-6